# Secondary and Quaternary Structures of the (+)-Pinoresinol-Forming Dirigent Protein†

Steven C. Halls and Norman G. Lewis*

*Institute of Biological Chemistry, Washington State University, Pullman, Washington 99164-6340*

*Received April 15, 2002*

ABSTRACT: The (+)-pinoresinol-forming dirigent protein is the first protein capable of stereoselectively coupling two coniferyl alcohol derived radical species, in this case to give the 8−8′ linked (+)-pinoresinol. Only dimeric cross-linked dirigent protein structures were isolated when 1-ethyl-3-[3-(dimethylamino)-propyl]carbodiimide was used as cross-linking agent, whereas the associated oxidase, presumed to generate the corresponding free radical substrate, was not detected. Native *Forsythia intermedia* dirigent protein isoforms were additionally subjected to MALDI-TOF and ESI-MS analyses, which established the presence of both monomeric masses of 23−25 kDa and dimeric dirigent protein species ranging from 46 to 49 kDa. Analytical ultracentrifugation, sedimentation velocity, and sedimentation equilibrium analyses of the native dirigent protein in open solution confirmed further its dimeric nature as well as a propensity to aggregate, with the latter being dependent upon both temperature and solution ionic strength. Circular dichroism analysis suggested that the dirigent protein was primarily composed of $\beta$-sheet and loop structures.

The lignan pinoresinol serves as a central precursor of many 8−8′ linked plant lignans, and is obtained by stereoselective coupling of two entities derived from *E*-coniferyl alcohol (Scheme 1). Its formation is of interest since it apparently employs two separate reactions: the first involves single-electron oxidation of coniferyl alcohol to form the corresponding phenoxy radical species via action of an oxidase/oxidant, whereas the second conversion is that of stereoselective radical−radical coupling to give (+)-pinoresinol (*1*). The protein employed for the stereoselective coupling step has been identified and its gene cloned, and the term dirigent protein (DP) (Latin: *dirigere*, "to guide or align") was coined to describe its mode of action (*1*−*4*). Although this coupling type is found only in a particular subset of 8−8′ linked lignans, it has been proposed that other DP and DP-like proteins exist and function in specific coupling reactions in the formation of other lignans (*4*−*7*). Moreover, the biosynthesis of other phenolic compounds, such as the biopolymeric lignins (*8*), the phenolic portion of suberins (*9*), as well as those deployed in insect cuticle melanization and sclerotization and in formation of phenolic polymers in fungal fruiting bodies (*10*), also involve bimolecular phenoxy radical coupling; control of their assemblies can be envisaged to utilize proteins containing dirigent sites (or arrays of dirigent sites) (*3*, *11*).

The DNA sequence of the (+)-pinoresinol DP from *Forsythia intermedia* implies an 18.3 kDa protein (*2*, *3*), whereas SDS−PAGE analysis of the native protein suggests an apparent molecular mass of 26 kDa (*1*); these differences result from glycosylation (*12*) and 4 potential *N*-glycosylation

Scheme 1: One-Electron Oxidation of Coniferyl Alcohol, and Effects on Coupling in the Presence and Absence of (+)-Pinoresinol-Forming Dirigent Protein

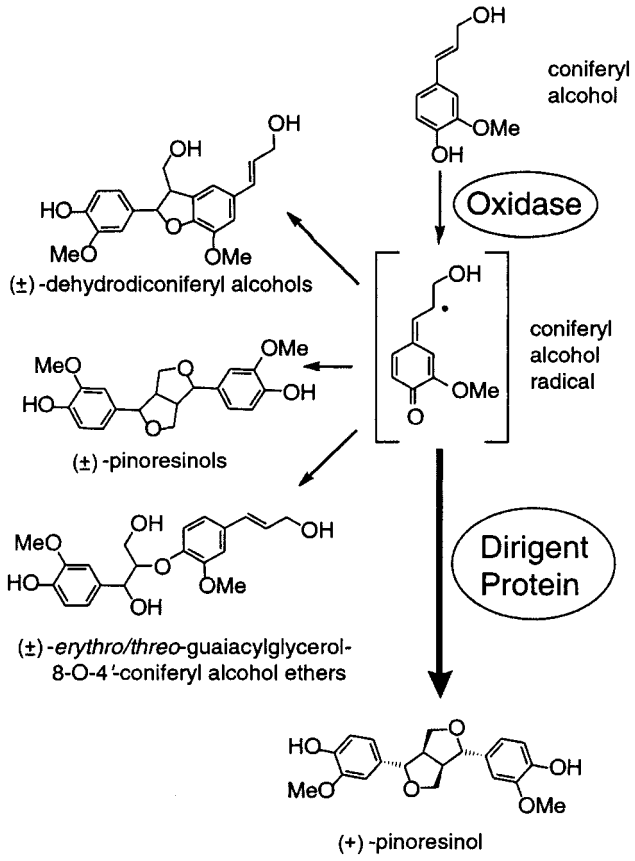


† This research was supported in part by the Lewis B. and Dorothy Cullman and G. Thomas Hargrove Center for Land Plant Adaptation, the United States Department of Energy (DOE) (DE-FG03-97ER20259), the DOE-National Science Foundation-United States Department of Agriculture funded Plant Biotechnology and Research Training Center (DE-FG06-94ER20160), and the National Science Foundation (MCB-9976684).

* Corresponding author. Telephone: (509) 335-8382. Fax: (509) 335-8206. E-mail: lewisn@wsu.edu.

10.1021/bi0259709 CCC: $22.00 
Published on Web 07/03/2002

sites have been identified. To date, there are over 200 other unique cDNA, ESTs, and genetic sequences in the databases with >70% homology and >40% identity to the (+)-pinoresinol DP; however, no additional specific functions have yet been described for the other gene products. Interestingly, homologues to (+)-pinoresinol DP from *Pisum sativum* (*13*) (56% identity, 74% homology) and *Nicotiana tabacum* (*14*) (48% identity, 70% homology) are inducible as part of a pathogen response.

On the basis of our current understanding of the stereoselective coupling process, the (+)-pinoresinol-forming DP appears to use coniferyl alcohol derived radical species as substrate. In vitro, the latter can be formed via action of any of a number of one-electron oxidants: this includes laccase, peroxidase, ammonium peroxydisulfate, and FMN radical generating systems (*1*). While no precise physiological role for any of these oxidases and/or oxidants has been identified for (+)-pinoresinol formation, it can be contemplated that a specific oxidase is proximal to the DP in vivo. In the absence of the DP, however, coniferyl alcohol radical species combine in vitro in open solution to produce (±)-dehydrodiconiferyl alcohols, (±)-pinoresinols, and *erythro*/*threo*-(±)-guaiacylglycerol coniferyl alcohol ethers in ratios of ~1:0.5:0.3, respectively (*1*) (Scheme 1).

The goal of this study was to characterize native (+)-pinoresinol-forming DP quaternary structure using cross-linking agents, and ESI and MALDI-TOF mass spectrometry to obtain accurate molecular masses. MALLS, GPC, and analytical centrifugation were also used to further support quaternary structural associations as well as in identifying hydrodynamic parameters and higher order associations, including that of possible aggregation. Additionally, far-UV circular dichroism analysis provided useful information on possible secondary structure.

## MATERIALS AND METHODS

*Protein Purification*. *F. intermedia* stems were harvested (September), following one year's annual growth of mature plants that were maintained in field plots at Washington State University. Purification of the (+)-pinoresinol-forming DP employed a procedure modified from that of Davin et al. (*1*), with all manipulations being carried out at 4 °C. Thus, frozen (−20 °C) *F. intermedia* stems (2 kg) were pulverized in a Waring blender (Model CB6) containing liquid $N_2$, with only powdered particles able to pass though an eight-mesh sieve being processed further. These were then sequentially extracted with acetone (3 × 4 L, −20 °C, 20 min) using a motorized impeller (250 rpm) for stirring, and following each extraction, the residue was retained by filtration through one layer of Miracloth (Calbiochem). To the resulting residue was added a solution of 1% Triton X-100 (v/v) in potassium phosphate buffer (0.1 M, pH 5.5, 8 L) containing 0.1% (v/v) $\beta$-mercaptoethanol, with the corresponding suspension being stirred (250 rpm) for 1 h and filtered as above. The residue was next treated with potassium phosphate buffer (0.1 M, pH 5.5, 8 L) with 0.1% (v/v) $\beta$-mercaptoethanol, then stirred (250 rpm) for 30 min, and filtered as before. A final extraction with NaCl (1.5 M) in potassium phosphate buffer (0.1 M, pH 5.5, 8 L), containing 0.1% (v/v) $\beta$-mercaptoethanol, was then stirred (250 rpm) for 1 h and again filtered. The filtrate from this last extraction step containing the DP was dialyzed against distilled water until a conductivity of <7 mS was achieved, and the resulting dialysate (8 L) was next filtered through a cotton plug in a 4 L funnel and subsequently through an α-cellulose (Sigma-Aldrich, filter aid, [9004-34-6]) packed bed (50 × 50 mm) before application to a 100 mL SP Sepharose Fast Flow (Amersham Pharmacia Biotech) column (50 × 55 mm, 30 mL $min^{-1}$) equilibrated in Na−Mes buffer (40 mM, pH 5.0). After washing with the same buffer, the sample was batch eluted with NaCl (2 M) in Na−Mes buffer (40 mM, pH 5.0, 500 mL), with the eluate frozen (−20 °C) until needed. An average of 10 batch eluates were thawed, pooled, concentrated (Amicon cell Model 2000, YM 30 membrane) to 500 mL, and precipitated with ammonium sulfate (40−80% saturation). The resulting precipitate was reconstituted in Na−Mes buffer (40 mM, pH 5.0, 100 mL), dialyzed against Na−Mes buffer (40 mM, pH 5.0, 3 × 4 L, 4 h), and applied (1 mL $min^{-1}$) to a MonoS HR5/5 column equilibrated in Na−Mes buffer (40 mM, pH 5.0, 100 mL). DP containing fractions were eluted (1 mL $min^{-1}$) stepwise between 233 and 333 mM $Na_2SO_4$ in 40 mM Na−Mes buffer, pH 5.0; these fractions were combined, diluted in Na−Mes buffer (20 mM, pH 5.0) until the conductivity was <7 mS, and then applied (10 mL $min^{-1}$) to a POROS SP column (4.6 × 100 mm) equilibrated in Na−Mes buffer (40 mM, pH 5.0). The DP was desorbed (5 mL $min^{-1}$) from the column using a linear $Na_2SO_4$ gradient from 0 to 250 mM in 20 mL, with the latter concentration being held constant for an additional 25 mL; the DP eluted with a conductivity ~30 mS. Apparent electrophoretic homogeneity of the DP, as evidenced by a single band on a silver stained SDS PAGE, was achieved after two further rounds of POROS-SP column chromatography following additional dilution of the eluate with Na−Mes buffer (40 mM, pH 5.0) to obtain a conductivity of <7 mS.

*General Assay Conditions*. Assay conditions were performed as previously described (*1*) using the following conditions: DP (40 nM), *E*-[9-$^3$H]-coniferyl alcohol (4 $\mu$M, 7 MBq $M^{-1}$), FMN (1 mM), Na−Mes buffer (40 mM, pH 5.0), and $Na_2SO_4$ (75 mM) in a total volume of 250 $\mu$L for 16 h at 30 °C with fluorescent room lighting. Extraction, separation, quantification, and determinations of the enantiomeric contents of the pinoresinols so formed were performed as previously described (*1*). Individual controls were carried out in the absence of DP, FMN, or both, or with samples which employed inactivated DP previously boiled in a water bath for 10 min.

*DP Polyclonal Antibody Affinity Column*. Polyclonal antibodies (5 mL serum), previously raised against the (+)-pinoresinol DP (*2*, *3*), were purified using ImmunoPure (Pierce) immobilized protein A/G resin (1 mL) following the manufacturer's protocol (*15*), including buffer exchange

[1] Abbreviations: CD, circular dichroism; DP, dirigent protein; EDC, 1-ethyl-3-[3-(dimethylamino)-propyl]carbodiimide; ESTs, expressed sequence tags; ESI-MS, electrospray ionization mass spectrometry; FMN, flavin mononucleotide; GPC, gel permeation chromatography; MALDI-TOF, matrix assisted laser desorbtion ionization time-of-flight; MALLS, multiangle laser light scattering; Na−Mes, NaOH buffered 2-(*N*-morpholino)ethanesulfonic acid; $M_w$, weight-average molecular mass; NBT/BCIP, nitro-blue tetrazolium chloride/5-bromo-4-chloro-3′-indolyphosphate *p*-toluidine salt; NHS, *N*-hydroxysuccinimide; PAGE, polyacrylamide gel electrophoresis; SDS, sodium dodecyl sulfate; TFA, trifluoroacetic acid.

through D-Salt columns. The corresponding purified antibodies (3 mL, 2.3 mg) were dialyzed against potassium phosphate buffer (50 mM, pH 7.5, 3 × 4 L, 6 h) to remove residual glycine. The antibodies in the solution were then attached to NHS-activated Sepharose (3.5 mL packed volume, Amersham Biosciences) using the manufacturer's protocol (*16*) with unreacted NHS groups blocked with trizma base (100 mM). Individual (0.5 mL, 5 × 25 mm) columns from this reaction were used to purify the cross-linked products below.

*Cross-Linking*. Two procedures were employed:

*Procedure 1*. The DP purification procedure was repeated as described above, except that a zero-length cross-linking agent EDC (8 mM) in a buffered solution (potassium phosphate buffer 0.1 M, pH 5.5, 8 L) was added to the homogenized powder (2 kg) prior to acetone extraction. After stirring (250 rpm, 1 h), the reaction was stopped by addition of $\beta$-mercaptoethanol (50 mM final concentration) and glycine (50 mM final concentration). A parallel extraction without cross-linking agent was also carried out. Extraction of the DP was then carried out as described above in Protein Purification. Samples in both cases were then taken as follows: the initial cross-linked solution containing EDC, the buffer solution following acetone extractions, and the extract obtained during NaCl solubilization. Each extract was next clarified by vacuum filtration through G6 glass fiber filters, then individually precipitated with ammonium sulfate (100% saturation), and resuspended in potassium phosphate buffer (40 mM, 100 mL, pH 7.5). The conductivity of each resulting solution was adjusted to ~20 mS by addition of solid NaCl.

Each protein resuspension was individually applied to the previously prepared antibody affinity column and eluted by the addition of 4 M urea (2 mL), with the eluate subsequently being subjected to a buffer exchange using a Sephadex G-25 column (14 × 50 mm) equilibrated in Na−Mes buffer (40 mM, pH 5.0). The various fractions so obtained were analyzed using western blot analysis with antibodies raised in a rabbit against the native *F. intermedia* DP probed with ImmunoPure goat antirabbit IgG (H + L) linked to alkaline phosphatase and visualized using 1-Step NBT/BCIP (Pierce).

*Procedure 2*. To a purified solution of DP (40 $\mu$g) in Na−Mes buffer (40 mL, 40 mM, pH 5.0, 20 °C) was added EDC to a concentration of 8 mM. After 30 min stirring, the reaction was stopped by addition of $\beta$-mercaptoethanol (50 mM final concentration) and glycine (50 mM final concentration). The solution was applied to a POROS R2 column (200 $\mu$L packed bed, 4 × 16 mm) equilibrated in Na−Mes buffer (40 mM, pH 5.0) and eluted with 300 $\mu$L $CH_3CN$:$H_2O$ (3:1, v/v), with 0.1% TFA in $H_2O$ (v/v). The resulting eluate was evaporated in vacuo, reconstituted, and visualized by western blot analysis as above.

*Extinction Coefficient*. The extinction coefficient of the DP was estimated in two ways. One approach employed the computational method of Gill and von Hippel (*17*) which utilizes the sequence of the native protein under denaturing (6 M guanidinium HCl) conditions, pH 6.5, 20 mM potassium phosphate buffer to give an extinction coefficient of 24 500 L mol$^{-1}$ cm$^{-1}$. The second was via direct quantitative measurement of the amino acids present in a DP protein solution of known absorbance. Samples were subjected to acid hydrolysis (6 N HCl, 100 °C, 30 h) and analyzed by a Beckman System 6300 amino acid analyzer using ion exchange separation and postcolumn ninhydrin quantification of each amino acid by comparison to standards, according to the manufacturer's protocol (*18*). Two replicates of the amino acids H, D + N, R, F, T, V, and K were quantified and averaged. [The common quantification of E + Q was not possible because a coeluting carbohydrate contaminant was present.] With the known sequence for comparison of amino acid composition, the extinction coefficient was thus calculated as 23 800 L mol$^{-1}$ cm$^{-1}$.

*GPC and MALLS*. This employed a TSK G3000SW (Tosoh Biosep, Montgomeryville, PA) column (7.55 × 600 mm) eluted with potassium phosphate buffer (50 mM, pH 5.0), containing NaCl (100 mM) at a flow rate of 1 mL min$^{-1}$ controlled by an Acuflow Series IV pump (Interfax Acuflow Ltd., Sutton Coldfield, UK). The eluate was monitored in series at 280 nm with a SSI 500 UV detector (Kyoto, Japan), an Optilab DSP (Wyatt Technology Corp.) interferometric refractometer, and a DAWN EOS system (Wyatt Technology Corp.) at room temperature. A calibration curve was obtained using horse heart cytochrome *c* (12.4 kDa), carbonic anhydrase (29 kDa), bovine serum albumin (66 kDa), alcohol dehydrogenase (150 kDa), $\beta$-amylase (200 kDa), and apoferritin (443 kDa) as standards. The extinction coefficient measured above was used to quantify the amounts of DP (300 $\mu$g) and to determine the concentration values which correlate the interferometer with the signals detected in the multiple angle light scattering device required for molecular mass determination as described by Wyatt (*19*). The $M_w$ value was calculated using the Debye method, extrapolating $R(\theta)/Kc$ to a zero value of $\sin^2(\theta)$. [$R(\theta)$ is the excess intensity of scattered light at angle $\theta$, $c$ is the sample concentration, $K$ is an optical parameter equal to $4\pi^2n^2$ (d$n$/d$c$)$^2/\lambda_o 4N_A$, $\lambda_o$ is the wavelength of scattered light, $n$ is the solvent refractive index, $dn$/d$c$ is the refractive index increment, and $N_A$ is Avogadro's number.]

*Analytical Ultracentrifugation*. All experiments were performed using a Beckman Optima XL-A analytical ultracentrifuge equipped with absorbance optics and an An60Ti rotor. Sedimentation equilibrium experiments were preequilibrated (1 h) at 20 °C and performed in Epon six channel (1.2 cm path) centerpieces at 6000, 9000, and 12 000 rpm monitored at 280 nm. Different DP concentrations (0.11, 0.33, and 1.0 mg mL$^{-1}$) were used in potassium phosphate buffer (20 mM, pH 5.0) containing NaCl (100 mM). The effects of NaCl on the DP were next examined at the same rotor speeds, temperature, and buffer with 0.5 mg mL$^{-1}$ DP and at NaCl concentrations of 0, 50, 100, 150, 250, and 500 mM at 20 °C. Data for 0.5 mg mL$^{-1}$ samples were also collected at 4, 6, 8, 10, 15, 20, 25, 30, 35, and 40 °C under the same rotor speeds with NaCl (100 mM). All samples were dialyzed (16 h) against the desired buffer conditions and used in the reference cell. Equilibrium profiles were analyzed with the program NONLIN (*20*), which is based on a nonlinear least squares technique fitting data to an approximation of the Lamm equation and capable of fitting multiple data sets simultaneously with different speeds and concentrations. Sedimentation velocity experiments were performed at 25 °C in Epon double channel centerpieces (1.2 cm path) with DP concentrations of 0.1, 0.2, 0.5, 0.67, 1.0, and 1.5 mg mL$^{-1}$ and at speeds of 25 000, 30 000, 36 000, and 45 000 rpm. Samples were previously dialyzed against

potassium phosphate buffer (20 mM, pH 5.0) containing 100 mM NaCl for 16 h. Sedimentation velocity data were collected at 280 nm with a radial increment of 0.2 mm and delay between scans of 800 s. Only data with a defined meniscus and plateau were analyzed by the Svedberg 5.01 (*21*, *22*) program using a modified Fujita-MacCosham function which fits sedimentation velocity profiles to an approximation of the Lamm equation, thereby allowing the determination of *D* and *s*. Molecular weight estimates were calculated from the values of *s* and *D* from the relation $M_w = sRT/D(1 - \bar{v}\rho)$, where *s* is the sedimentation coefficient, *R* the gas constant, *T* the temperature, *D* the diffusion coefficient, $\bar{v}$ the partial specific volume, and $\rho$ the solvent density. The partial specific volume ($\bar{v}$) of the DP was calculated to be 0.710, from the amino acid composition using the method of Cohn and Edsall (*23*), assuming that all glycosylation consistently had the partial specific volume of glucose, and temperature effects were corrected according to Durchschlag (*24*).

*CD*. The far-UV spectra of the DP were collected from a AVIV stopped flow circular dichroism spectrophotometer (Model 2025F) (Lakewood, NJ) at 20 °C in a 0.1 cm cell with DP concentrations of 7, 10, and 20 $\mu$M in Na−Mes buffer (40 mM, pH 5.0). The spectra were compared to several library sets (*25*) of known secondary structures using the programs CDSSTR (*26*), SELCON3 (*27*), and CONTIN (*28*).

*MALDI-TOF Mass Spectrometry*. DP samples were diluted to 5−10 pmol in $H_2O$ (0.4 $\mu$L) and mixed with an equal volume of a saturated aqueous solution of sinapinic acid as matrix. A Voyager DE\RP mass spectrometer with a PerSeptive Biosystems Voyager Biospectrometry Workstation was used with data analyzed using the Data Explorer 5.1 software package. Laser fluence was about 20% above threshold, and the collected spectra were from 256 scans. Mass standards of cytochrome *c* (12 360 Da) and trypsinogen (23 980 Da) were used for instrument calibration.

*ESI-MS*. An aqueous solution of DP (100 pmol) in 10 $\mu$L was applied to a Waters Symmetry Shield $C_{18}$ (3.5 $\mu$m, 1.0 × 150 mm) column using a Waters 2690 Alliance Separation module. The column was equilibrated with solvents A ($CH_3$-CN, Burdick and Jackson, High Purity Solvent) and B ($H_2O$: $HCO_2H$, EM Science, Suprapur, 99:1) at a ratio of (5:95) and eluted with a linear gradient of A:B (5:95 to 70:30) in a 40 min period with a flow rate of 50 $\mu$L min$^{-1}$. Mass spectroscopic analysis of the effluent was performed in-line with a Finnigan-Thermoquest LCQ equipped with an electrospray ionization source and ion trap detector. Other operating parameters included 60 (arbitrary units) as the sheath gas flow rate, and a capillary temperature of 200 °C. Mass spectra were deconvoluted using the software package BioExplore (Finnigan Corp.).

## RESULTS AND DISCUSSION

*DP Quaternary Structure.* The modified protocol for DP purification significantly improved recoveries relative to that of the previously reported method; this provided approximately 50 $\mu$g of purified DP per kg fresh *F. intermedia* stem tissue, an 80% improvement in yield with only 20% of the labor of the previous method (*1*). Next, cross-linking/immunoprecipitation, using the cross-linking agent EDC, was utilized in order to reveal potential associations of the (+)-pinoresinol-forming complex, i.e., either between individual DP monomers and/or between the DP and an auxiliary oxidase. [EDC is a carbodiimide-based zero-length cross-linker which forms an amide linkage between amines and carboxylic acid groups (*29*).]

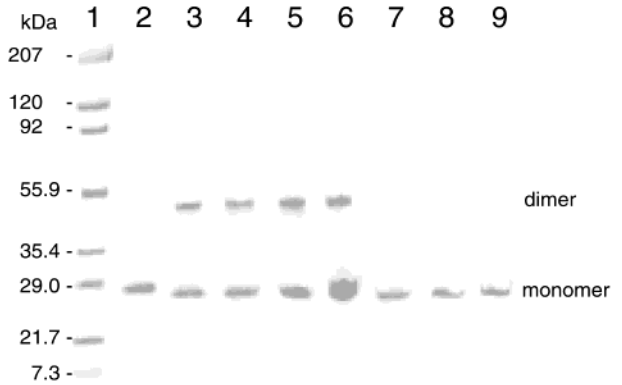


FIGURE 1: Western blot analysis of various *F. intermedia* extracts separated on an SDS−PAGE gel, using polyclonal antibodies raised against the (+)-pinoresinol-forming dirigent protein from *F. intermedia*. (lane 1) Molecular weight standards (prestained). (lane 2) Purified native dirigent protein. (lane 3) Purified native dirigent protein following EDC cross-linking. (lanes 4−6) After cross-linking, samples for western blot analysis were taken at different stages of DP purification as follows: (4) soluble protein extract, (5) buffered extract following acetone washes, (6) final NaCl solubilization extract (see Materials and Methods). (lanes 7−9) The same as lanes 4−6, but without EDC cross-linking.

Cross-linking was carried out both prior to solubilization of the (+)-pinoresinol-forming system, as well as with purified preparations (see Materials and Methods). None of these manipulations, however, resulted in detection of any cross-linking between the DP and an oxidase moiety. On the other hand, a presumed cross-linked DP dimeric species ~50 kDa (Figure 1, lanes 3−6) was detected along with the monomer (~26 kDa), as revealed by western blot analysis of the SDS−PAGE gel. With control experiments (no EDC treatment), only the denatured monomer was observed (lanes 2,7−9). Furthermore, while previous investigations had demonstrated that measurable (+)-pinoresinol-forming capacity was essentially only found in the NaCl solubilized extract from *F. intermedia* stem tissue (lanes 6,9), the western blot analyses indicated that some level of DP could be detected in the initial buffered solubilization (lanes 3,7) and extracts following Triton X-100 (lanes 4,8); the relative amounts, however, were not determined.

*ESI-MS and MALDI-TOF-MS Analyses.* The ESI-MS spectrum of the native DP, with multiple charges indicated in parentheses (Figure 2A), was deconvolved from the multiple *m*/*z* states to the corresponding mass (Figure 2B); this resulted in detection of both a single monomer (24 748 mass units) and the corresponding dimer (49 501 mass units). Two other potential dimeric species were also observed at 47 962 and 46 569 mass units, these perhaps representing entities that have either lost or which contain modified glycosyl residues. MALDI-TOF analysis, on the other hand, gave a broader mass range of peaks centered at ~23 129−23 501 *m*/*z*, (Figure 2C) and a doubly charged range centered ~11 571−11 726 *m*/*z*. Thus, both ESI and MALDI-TOF mass spectrometric analyses indicated that the DP monomeric species is greater than the 18.3 kDa protein expected from

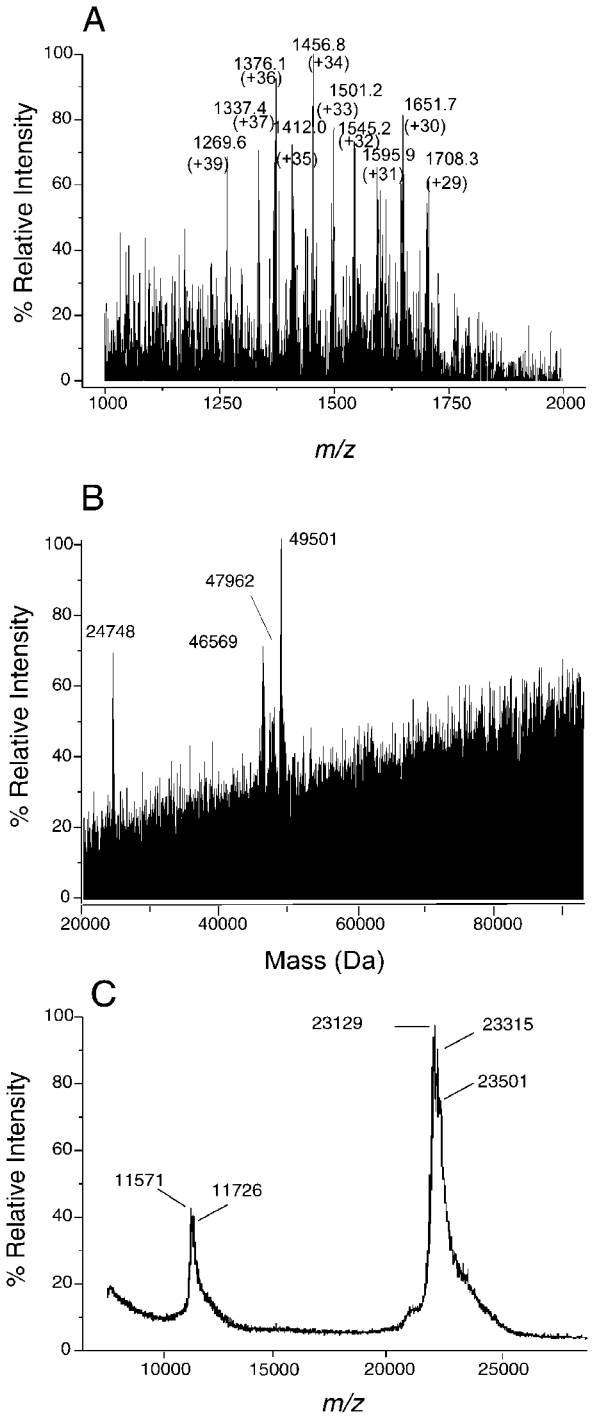


FIGURE 2: ESI and MALDI-TOF mass spectra of native purified (+)-pinoresinol-forming dirigent protein from *F. intermedia*. (A) ESI-MS multiple charge envelope. (B) Deconvolution of multiple charge envelope, A, with both monomeric and dimeric components labeled. (C) MALDI-TOF spectrum, showing both singly and doubly charged monomer masses.

the DNA coding sequence with a dimeric form detectable by ESI-MS.

*Gel Permeation Chromatography−MALLS.* Comparing the DP elution profile to that of reference standards (see Materials and Methods) using a TSK G3000SW column matrix, we estimated a molecular weight of ~53 kDa. GPC-MALLS was then also employed to estimate the native DP $M_w$; however, prior to this measurement, the extinction coefficient of the (+)-pinoresinol-forming DP was first

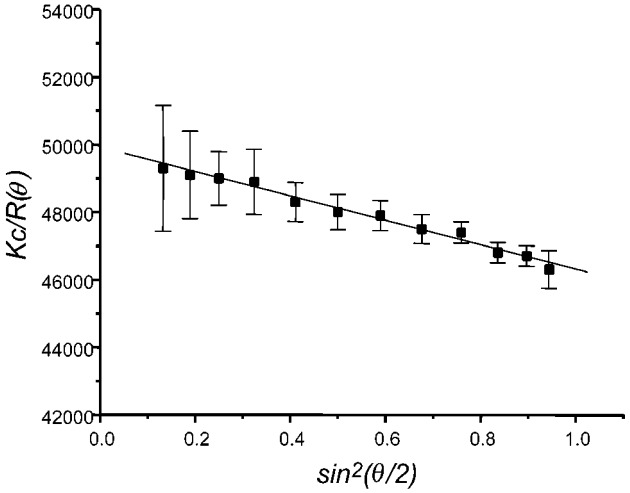


FIGURE 3: Debye plot of the *F. intermedia* (+)-pinoresinol-forming DP following MALLS analysis. This was calculated from a selected point of the native DP elution peak obtained during GPC using a TSK G3000SW column. *R*, intensity of scattered light; *K*, an optical parameter; *c*, concentration; $\theta$, scattering angle (see Materials and Methods).

calculated (see Materials and Methods) with the value of 24 500 L $mol^{-1}$ $cm^{-1}$ being utilized. In this way, a Debye plot was calculated for the (+)-pinoresinol-forming DP (Figure 3), using a single time point near the GPC DP peak maximum. Extrapolation of $R(\theta)/Kc$ to zero (see Materials and Methods) thus indicated that the native DP has a weight average molar mass ($M_w$) of 49.9 ± 1.6 kDa for the dimer. Interestingly, these estimates of $M_w \sim 53$ and 49.9 kDa differ from that previously obtained using Sephacryl S300, which suggested a $M_w \sim 78$ kDa for the DP (*1*). The latter data are rationalized as being a consequence of nonideal elution behavior of the glycosylated DP on the S300 matrix.

*Ultracentrifugation.* DP samples were next sedimented at three velocities, whose sedimentation profiles were monitored by UV absorbance (280 nm) at various time intervals (see Figure 4A for a representative sedimentation profile). It was found that the DP sedimented with a $s_{20,w}$ of $3.52 \times 10^{-13}$ s with a diffusion constant, *D*, of $7.2 \times 10^{-7}$ $cm^2$ $s^{-1}$, which corresponds to a dimeric $M_w$ of 46.7 kDa using the calculated $\bar{v}$ of 0.710 for the native DP.

Interestingly, when the native DP was allowed to stand unperturbed for ~16 h prior to sedimentation analysis about 37% of the total DP formed an aggregate (Figure 4B). That is, under these conditions, both a slowly sedimenting species corresponding to the DP dimer was observed as well as an aggregate with a $s_{20,w}$ of $1.8 \times 10^{-12}$ s and a large diffusion constant ($2.5 \times 10^{-6}$ $cm^2$ $s^{-1}$). Moreover, the data indicated that the larger molecular weight species was an ensemble of aggregates in the range of 300−450 kDa (12−18-mer), an observation consistent with sedimentation equilibrium data (data not shown). However, this aggregation behavior could be prevented by increasing NaCl concentration and to a lesser extent by increasing temperature (data not shown).

Utilizing the ESI-MS $M_w$ of ~49.5 kDa (considered to be the most accurate value) for the DP dimer, a more precise hydrodynamic analysis of DP dimer shape was also estimated using the Teller method (*30*). This suggested that the DP has a Stokes radius, $R_o$, of 2.5 nm and is slightly anisotropic, with one axis having a maximum radius of 3.2 nm and the

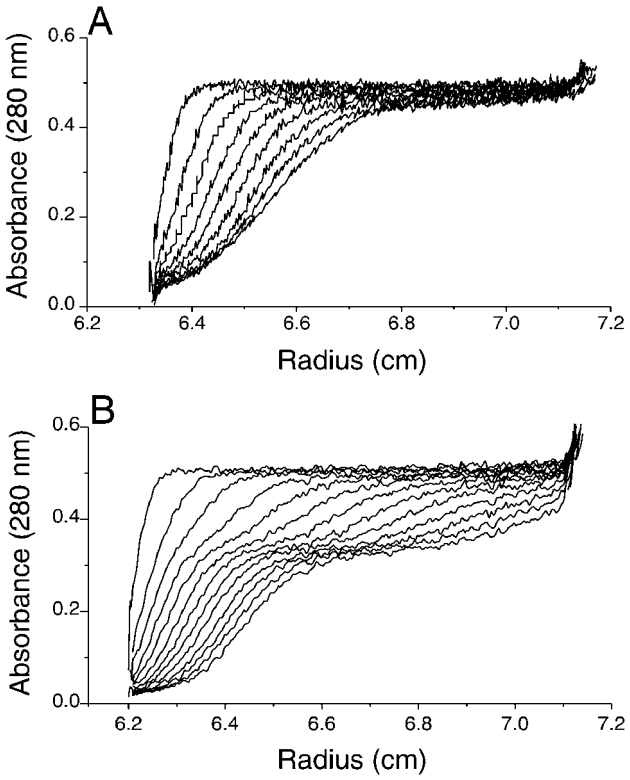


FIGURE 4: Sedimentation velocity absorbance profiles of native *F. intermedia* dirigent protein. (A) Freshly prepared protein. Consecutive traces are 1092 s apart in time, the first trace is at 1047 s, being recorded at 20 °C and 36 000 rpm. (B) Sedimentation velocity absorbance profile of native *F. intermedia* dirigent protein illustrating presence of a dimeric and a rapidly sedimenting component (12−18-mer) following storage for 16 h. Consecutive traces are 800 s apart in time, the first trace, is at 293 s, 20 °C, and 36 000 rpm.

other a minimum of 2.2 nm. In agreement with this, a radius of gyration, $R_g$, was also calculated to be 2.2 ± 0.5 nm from analysis of the Debye plot (*19*).

*CD.* Finally, since the aggregation behavior of the purified DP suggested that it may be predominantly of $\beta$-protein character, a circular dichroism analysis was next carried out to ascertain if this was the case. Figure 5 shows the corresponding CD spectrum with a superimposed calculation of the best fit of various secondary structural features. These data indicated that the DP was composed of 40−47% loop, 35−42% $\beta$-sheet, 9−14% turn, and 5−12% α-helix structure. This corresponds well with secondary structure predictions given by most computer algorithms (*31*−*34*), which uniformly predict nine $\beta$-sheet regions (11−20, 32−36, 55−59, 79−83, 90−98, 108−113, 123−126, 137−141, 148−161) within the protein, as well as a possible single α-helix (130−135) and ∼50% loop structure.

*Concluding Remarks.* Application of a cross-linking strategy using EDC, as well as ESI-MS, MALDI-TOF-MS, GPC-MALLS, and ultracentrifugation, confirmed that the primary molecular form of the native (+)-pinoresinol-forming DP was a dimer of ∼50 kDa: no cross-linking of a DP-oxidase complex was observed under the conditions employed. Analytical ultracentrifugation also indicated a propensity for the DP to aggregate, and a CD analysis suggested that it was mainly of $\beta$-sheet character, thereby provisionally providing an explanation for the propensity to aggregate. Additionally, it is our current working hypothesis

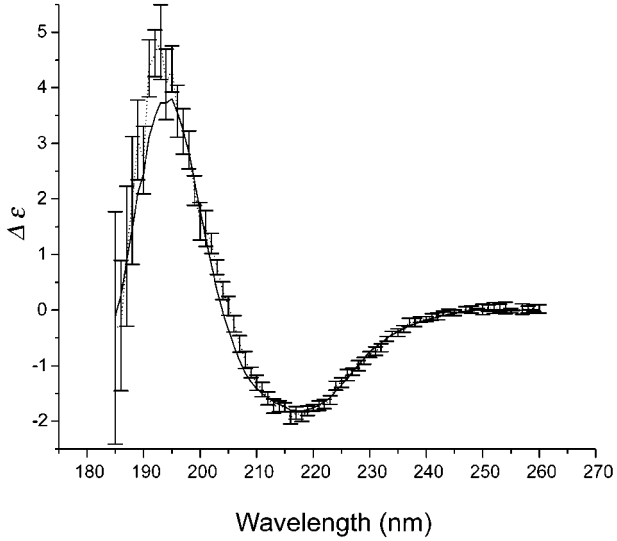


FIGURE 5: CD spectrum of *F. intermedia* (+)-pinoresinol-forming DP measured at three concentrations and averaged. An expected fit (solid) to the observed CD spectrum (dashed) is shown for a protein with secondary structural components of 40−47% loop, 35−42% $\beta$-sheet, 9−14% turn, and 5−12% α-helix.

that the (+)-pinoresinol-forming DP contains one dirigent (coniferyl alcohol radical) binding site per protein monomer. Thus, the presence of the dimer enables each substrate monomer to be oriented such that 8−8′ bond formation occurs via coupling between the two *si*−*si* faces of each substrate molecule. In the future, how binding is precisely effectuated will be determined using, for example, X-ray crystallographic analysis.

## ACKNOWLEDGMENT

The authors thank Dr. Lisa Gloss, Dr. ChulHee Kang, and HaJeung Park for assistance in operating the AVIV circular dichroism spectrophotometer and the Wyatt dynamic light scattering instrument, respectively, and Dr. Gerhard Munske for performing amino acid analysis.

## REFERENCES

1. Davin, L. B., Wang, H.-B., Crowell, A. L., Bedgar, D. L., Martin, D. M., Sarkanen, S., and Lewis, N. G. (1997) Stereoselective bimolecular phenoxy radical coupling by an auxiliary (dirigent) protein without an active center, *Science 275*, 362−366.
2. Gang, D. R., Costa, M. A., Fujita, M., Dinkova-Kostova, A. T., Wang, H.-B., Burlat, V., Martin, W., Sarkanen, S., Davin, L. B., and Lewis, N. G. (1999) Regiochemical control of monolignol radical coupling: a new paradigm for lignin and lignan biosynthesis, *Chem. Biol. 6*, 143−151.
3. Burlat, V., Kwon, M., Davin, L. B., and Lewis, N. G. (2001) Dirigent proteins and dirigent sites in lignifying tissues, *Phytochemistry 57*, 883−897.
4. Lewis, N. G., and Davin, L. B. (1999) Lignans: biosynthesis and function, in *Comprehensive Natural Products Chemistry* (Barton, Sir D. H. R., Nakanishi, K., and Meth-Cohn, O., Eds.) Vol. 1, pp 639−712, Elsevier, London.
5. Lewis, N. G., Davin, L. B., and Sarkanen, S. (1998) Lignin and lignan biosynthesis: distinctions and reconciliations, in *Lignin and Lignan Biosynthesis* (Lewis, N. G., and Sarkanen, S., Eds.) Vol. 697, pp 1−27, ACS Symposium Series, American Chemical Society, Washington, DC.
6. Davin, L. B., and Lewis, N. G. (2000) Dirigent proteins and dirigent sites explain the mystery of specificity of radical precursor coupling in lignan and lignin biosynthesis, *Plant Physiol. 123*, 453−461.
7. Wang, C.-Z., Davin, L. B., and Lewis, N. G. (2001) Stereoselective phenolic coupling in *Blechnum spicant*: formation of 8-2′ linked

(−)-*cis*-blechnic, (−)-*trans*-blechnic and (−)-brainic acids, *J. Chem. Soc., Chem. Commun.* 113−114.
8. Nose, M., Bernards, M. A., Furlan, M., Zajicek, J., Eberhardt, T. L., and Lewis, N. G. (1995) Towards the specification of consecutive steps in macromolecular lignin assembly, *Phytochemistry 39*, 71−79.
9. Bernards, M. A., Lopez, M. L., Zajicek, J., and Lewis, N. G. (1995) Hydroxycinnamic acid-derived polymers constitute the polyaromatic domain of suberin, *J. Biol. Chem. 270*, 7382−7386.
10. Bu'Lock, J. D., Leeming, P. R., and Smith, H. G. (1962) Pyrones. Part II. Hispidin, a new pigment and precursor of a fungus "lignin", *J. Chem. Soc.* 2085−2089.
11. Lewis, N. G., Davin, L. B., and Sarkanen, S. (1999) The nature and function of lignins, in *Comprehensive Natural Products Chemistry* (Barton, Sir D. H. R., Nakanishi, K., and Meth-Cohn, O., Eds.) Vol. 3, pp 617−745, Elsevier, London.
12. Lewis, N. G., and Davin, L. B. (1998) The biochemical control of monolignol coupling and structure during lignan and lignin biosynthesis, in *Lignin and Lignan Biosynthesis* (Lewis, N. G., and Sarkanen, S., Eds.) Vol. 697, pp 334−361, ACS Symposium Series, American Chemical Society, Washington, DC.
13. Choi, J. J., Klosterman, S. J., and Hadwiger, L. A. (2001) A comparison of the effects of DNA-damaging agents and biotic elicitors on the induction of plant defense genes, nuclear distortion, and cell death, *Plant Physiol. 125*, 752−762.
14. Schreier, P., Garbers, C., Langen, G., and Kiedrowski, S. (1999) Tobacco cDNAs for genes induced upon pathogen infection and their uses, German Patent DE19813048 Bayer A.G.
15. Pierce Chemical (1999) *Instruction Manual 20421*, Rockford IL.
16. Amersham. Biosciences Inc. (1999) *Instruction Manual 71-5000-14*, Upsala, Sweden.
17. Gill, S. C., and von Hippel, P. H. (1989) Calculation of protein extinction coefficients from amino acid sequence data, *Anal. Biochem. 182*, 319−326.
18. Beckman (1985) *System 6300 Amino Acid Analyzer Manual*, Fullerton, CA.
19. Wyatt, P. J. (1993) Light scattering and the absolute characterization of macromolecules, *Anal. Chim. Acta 272*, 1−40.
20. Johnson, M. L., Correia, J. J., Yphantis, D. A., and Halvorson, H. R. (1981) Analysis of data from the analytical ultracentrifuge by nonlinear least-squares techniques, *Biophys. J. 36*, 575−588.
21. Philo, J. S. (1992) *Svedberg 5.01*, Amgen Inc., Thousand Oaks, CA.
22. Philo, J. S. (1997) An improved function for fitting sedimentation velocity data for low-molecular-weight solutes, *Biophys. J. 72*, 435−444.
23. Cohn, E. J., and Edsall, J. T. (1943) *Proteins, Amino Acids and Peptides as Ions and Dipolar Ions*, Rheinhold, New York.
24. Durchschlag, H. (1986) in *Thermodynamic Data for Biochemistry and Biotechnology* (Hinz, H.-J., Ed.) pp 45−128, Springer-Verlag, New York.
25. Sreerama, N., and Woody, R. W. (2000) Estimation of protein secondary structure from circular dichroism spectra: comparison of CONTIN, SELCON, and CDSSTR methods with an expanded reference set, *Anal. Biochem. 287*, 252−260.
26. Johnson, W. C. (1999) Analyzing protein circular dichroism spectra for accurate secondary structures, *Proteins 35*, 307−312.
27. Sreerama, N., and Woody, R. W. (1993) A self-consistent method for the analysis of protein secondary structure from circular dichroism, *Anal. Biochem. 209*, 32−44.
28. Provencher, S. W., and Glockner, J. (1981) Estimation of globular protein secondary structure from circular dichroism, *Biochemistry 20*, 33−37.
29. Hermanson, G. T. (1996) *Bioconjugate Techniques*, Academic Press, San Diego, CA.
30. Teller, D. C. (1976) Accessible area, packing volumes, and interaction surfaces of globular proteins, *Nature 260*, 729−731.
31. Kneller, D. G., Cohen, F. E., and Langridge, R. (1990) Improvements in protein secondary structure prediction by an enhanced neural network, *J. Mol. Biol. 214*, 171−182.
32. Rost, B. (1996) PHD: predicting one-dimensional protein structure by profile-based neural networks, *Methods Enzymol. 266*, 525−539.
33. Rost, B., and Sander, C. (1993) Prediction of protein secondary structure at better than 70% accuracy, *J. Mol. Biol. 232*, 584−599.
34. Rost, B., and Sander, C. (1994) Combining evolutionary information and neural networks to predict protein secondary structure, *Proteins 19*, 55−72.

BI0259709